Enhanced Self-Assembly of Metal Oxides and Metal-Organic Frameworks from Precursors with Magnetohydrodynamically Induced Long-Lived Collective Spin States

Eric Breynaert, Jens Emmerich, Danilo Mustafa, Sneha R. Bajpe, Thomas Altantzis, Kristof Van Havenbergh, Francis Taulelle, Sara Bals, Gustaaf Van Tendeloo, Christine E. A. Kirschhock,* and Johan A. Martens*

Molecular assembly involves the self-organization of pre-existing chemical subunits into larger, ordered structures.[1] Self-organization can be driven by cooperative interaction among subunits with or without aid of externally induced forces.[2,3] Dynamic phenomena and transient interactions or shapes play an important role in self-assembly processes involving high energy dissipation.[4,5] Literature provides examples of self-assembly processes in magnetic fields.[6,7] Grzybowski et al. demonstrated a magnetic energy dissipative system generating high degrees of order from a disordered set of macroscopic paramagnetic discs floating at an air/water interface.[8] The rotation of an external magnetic field below the system forced the discs to self-organize into a hexagonal pattern of auto-rotating monomeric units as result of the competition between the magnetic and auto-rotation induced hydrodynamic forces. On a molecular scale, Coey et al. demonstrated how a permanent magnetic field (1T) can be used to create a self-contained tube of concentrated paramagnetic electrolyte solution flowing inside a solution of ultra-pure water.[9,10]

These examples demonstrate how the application of a static, external magnetic field on moving magnetic or electric dipoles (or vice versa) results in an accumulation of forces comprising the Lorenz force, field induced internal electric currents generating an opposing magnetic force and the hydrodynamic forces. In case of electrolyte solutions containing paramagnetic ions (charged magnetic dipoles) the resulting effective magnetic and electric fields are extremely complex, but still can be tuned to either suppress or augment convection and dispersion of paramagnetic ions in the solvent.[9]

Dr. E. Breynaert, Dr. J. Emmerich, Dr. D. Mustafa, Dr. S. R. Bajpe, Prof. F. Taulelle, Prof. C. E. A. Kirschhock, Prof. J. A. Martens
KU Leuven – Center for Surface Chemistry and Catalysis (COK)
Kasteelpark Arenberg 23 – box 2461
B-3001, Heverlee, Belgium
E-mail: eric.breynaert@biw.kuleuven.be; christine.kirschhock@biw.kuleuven.be

T. Altantzis, K. Van Havenbergh, Prof. S. Bals, Prof. G. Van Tendeloo
University of Antwerp - Electron Microscopy for Materials Research (EMAT)Groenenborgerlaan 171, B-2020, Antwerp, Belgium

DOI: 10.1002/adma.201400835

The external forces acting on a flow of charged species can be controlled by guiding the flow through a restriction in a hydrodynamic (HD) system, with a permanent magnetic field perpendicular to the flow direction, the so-called magneto-hydrodynamic (MHD) system.[10] MHD treatment with weak magnetic field has already been demonstrated to assist in formation of monodisperse emulsions,[11] in nano-aggregate breakup,[12,13] and in Mo-V-Sb mixed oxide catalyst synthesis.[14]

This manuscript reports on a new type of MHD-induced phenomenon dramatically and permanently affecting self-organization and magnetic structure of spin-ice, spin-glass or spin-liquid materials during wet-chemical synthesis. This effect is demonstrated by application of a weak permanent magnetic field (ca. 0.3 T) during synthesis of vanadium oxide nano-scrolls, manganese oxide nano-tubes and COK-16, a polyoxometalate encapsulating HKUST-1 type MOF in a magneto-hydrodynamic device. The presented MHD system enables precise variation of the nonlinear flow-magnetic field dynamics by controlling the MHD parameters – flow and field.[15] Since the beneficial effects induced in the example materials are likely to occur in many systems, MHD synthesis of technologically advanced materials is expected to both represent significant economic value, and deepen the mechanistic understanding of dynamical self-assembly processes.[16,17]

Manganese Oxide Nanorods: Manganese oxide nanorods are rod-like morphologies of the 2 × 2 tunnel oxide hollandite, which are commonly synthesised by chemical reduction of dissolved permanganate followed by hydrothermal treatment.[18] In presence of K^+ cations, prolonged hydrothermal treatment converts the initially dense nanorods (diameter: 100 nm) into hollow nanotubes with a wall thickness of 30 nm via a chemical etching process.[19] Post-synthesis modifications changing the K^+ content in the 2 × 2 tunnel cavity allows tuning of the magnetic properties α-MnO_2 nanotubes by alteration of the distribution of Mn^{3+} and Mn^{4+} ions on the triangular lattice of the Kagomé oxide α-K_xMnO_2. Above x = 0.1 the geometrical frustration of the spins leads to spin glass behaviour.[20]

Preparation of K^+ doped α-MnO_2 nanorods by hydrothermal treatment of a hydrodynamically mixed synthesis suspension (HCl + $KMnO_4$)[21] resulted in whorled, rodlike MnO_2 nanocrystals with poorly defined morphology and plenty of surface defects in the form of ongrown secondary crystallites. The magnetohydrodynamic turbulent conditions induced by

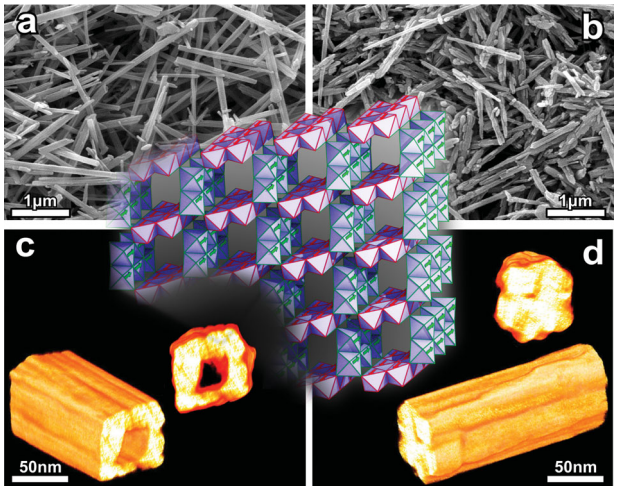

Figure 1. MnO_2 nanotubes after hydrothermal treatment, obtained from reaction mixtures pretreated in presence (a,c) and absence (b,d) of an external magnetic field (B = 0.3 T). a and b: SEM images, c and d: Electron tomography reconstruction showing the particle morphology along different viewing directions. The inset (center) illustrates the crystal structure of α-MnO_2. The differently colored octahedra symbolise opposite alignment of the magnetic moments.

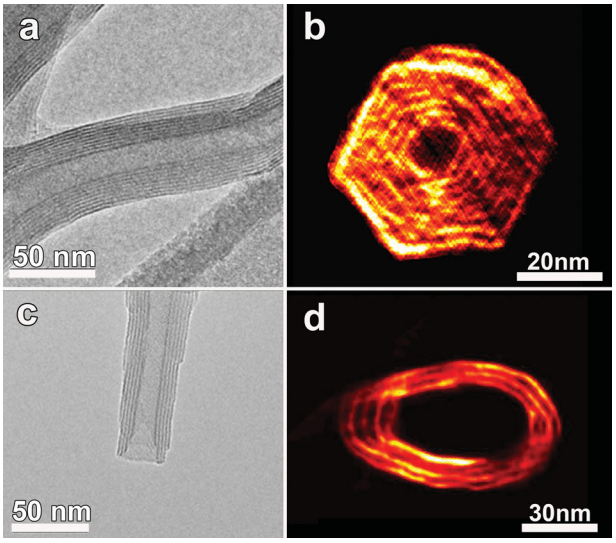

Figure 2. Conventional transmission electron microscopy images of vanadium oxide nanotubes (VOx-NTs) obtained after hydrothermal aging of precursor gels pretreated with MHD and HD are presented in Figure 3 a and c respectively. These images only correspond to 2 dimensional projections of 3 dimensional objects. Therefore, electron tomography was used and cross sectional slices through the (3 dimensional) reconstructed volume are presented in Figure 3 b and d. Note the improved ordering and increased layer stacking in the tube walls, highlighted by a well-defined hexagonal cross-section of the tube compared to a rather tubular, oligo-layered cross-section of the sample derived from HD pretreated gels.

addition of a weak magnetic field (0.3 T) perpendicular to the flow in the HD device resulted in the improved self-assembly of nanotubes during hydrothermal treatment. As shown in **Figure 1**, the MHD pre-treatment induces the formation of well-defined hollow MnO_2 nanotubes, increases yield (> 5-fold increase) and crystallinity, suppresses formation of non-tubular crystals and surface-nucleation (Scanning EM, Transmission EM, PXRD; see Figures S1 and S2). As shown by Luo et al., the growth process of these hollow nanotubes involves initial self-assembly of dense nanorods, followed by chemical etching of the inner core. This process was shown to be highly dependent on the spin order in the structure,[19,20] and can be correlated with the dissolution of an anti-ferromagnetic inner core of α-MnO_2 (hollandite), in favour of an α-K_xMnO_2 (cryptomelane) shell with spin glass behaviour.[19,20,22] Therefore it can be hypothesized that the MHD turbulent conditions applied during pre-treatment induce a long lived state of collective spin order by the resonant coupling of magnetic field and turbulent structured flow (Couette type). The internal spin order of the nanoscopic building units consequently improves self-assembly and induces formation of perfectly aligned, hollow nanotubes, without any need for etching dense nanorods.

Vanadium Oxide Nanoscrolls: Vanadium oxide nanoscrolls can be synthesized from brightly yellow layered vanadium pentoxide. During the first stages of the synthesis, the layered V_2O_5 is intercalated with organic amine templates at room temperature.[23] During intercalation, diamagnetic V^{+5} is partially reduced to paramagnetic V^{+4}, a process accompanied with a progressive change in color from bright yellow via orange to deep brown-red, caused by the formation of a precursor with polarons that are mobile within the vanadium sheets. This precursor is best described as spin liquid system.[23,24] Upon hydrothermal treatment of this deep red precursor gel,[23] the mixed octahedral/tetrahedral layers flex to form vanadium nanoscrolls from alkylamine[VO_x] sheets, closely related to the structure observed in TMA[V_4O_{10}].[25] In a synthesis combining a stirred pre-treatment with the hydrothermal treatment non-uniform scrolls with low degrees of order of the scrolling are obtained. MHD treatment strongly enhances precursor formation resulting in deep red gels after 3 h of MHD treatment as compared to 6 h of pure HD treatment. Furthermore, MHD pre-treatment drastically improves intra- and inter-layer order, which upon hydrothermal treatment leads to unprecedented hexagonally scrolled materials (**Figure 2**). Commeinhes et al. demonstrated with polarized-light microscopy how application of a weak permanent field orients the nanoribbons comprising nematic vanadium pentoxide gels to form one single magnetic domain.[26] Translated to the MHD turbulent conditions prevailing during MHD pretreatment of the nanoscroll synthesis gel, the local formation of magnetic domains implies an alignment of the spins within and between neighbouring VO_x nanosheets during their presence in the magnetic field. This increase in correlation time can allow unpaired electron spins to evolve into weakly coupled electron spin structures.[27] The hexagonal scrolling can easily be rationalised considering the construction of the V_2O_5 sheets with chains of vanadium square pyramids (SP) with their apexes alternating up (U) and down (D) while sharing two neighbouring edges of the base. These UD chains share SP corners in such a way that they can be transformed to each other by a 120° rotation along a chiral 3-fold axis. Related structures are for example found in V_nO_{2n+1} hexagonal tunnel frameworks such as $Cs_{0.3}V_2O_5$ and $Cs_{0.35}V_3O_7$.[28]

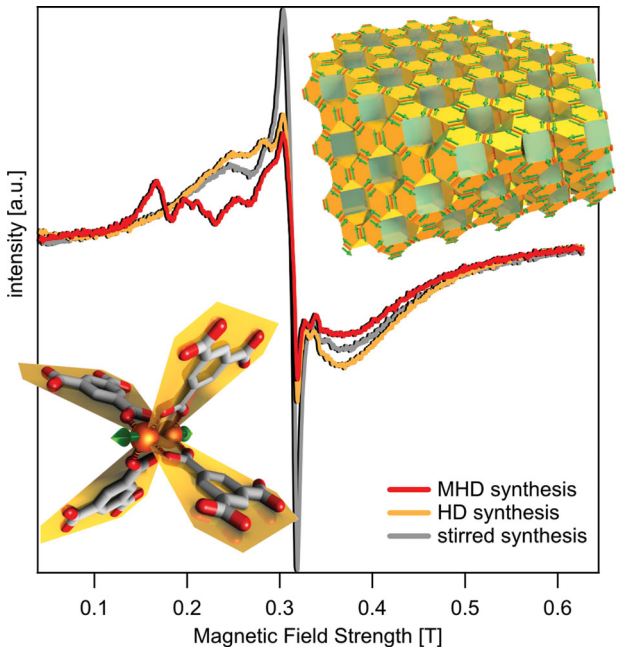

Figure 3. Room temperature EPR spectra of COK-16 for a stirred, hydrodynamic (HD) and magneto-hydrodynamic (MHD) synthesis using a static magnetic field of 0.3 T. Measurements at 140 K are provided in the supplementary material (Figure S1). The inset on the left shows a Cupaddle wheel, the basic building block of the structure. The one on the right provides a general view of the COK-16 structure, where the Cu-pairs are arranged in a Kagomé lattice[32] in the 111 planes. Green arrows illustrate the alignment of the magnetic moments.

Metal Organic Framework COK-16: In case of polyoxometalate encapsulated metal organic framework COK-16,[29,30] magneto hydrodynamic (MHD) synthesis results in the appearance of a double quantum excitation in the electron paramagnetic resonance (EPR) spectrum (**Figure 3**) without changing the framework structure, according to X-ray Diffraction (XRD) (Figure S3). These double quantum excitations (DQ) are typically observed when magnetic dipole/dipole coupling between Cu^{2+} sites or Cu^{2+} pairs gain importance, relative to the direct exchange or super-exchange coupling in the pairs. The rate limiting reaction steps in the synthesis of HKUST-1 type MOFs such as COK-16 is the conversion of isolated, paramagnetic Cu^{2+} ions into diamagnetic Cu_2^{4+} pairs in paddle wheels (Figure 3, inset left). Antiferromagnetic (AF) coupling between the Cu^{2+} spins in the paddle wheel occurs via a super-exchange mechanism. Comparison of the quantitative EPR spectra for COK-16 synthesized in presence and absence of magnetic fields (Figure 3) indicates significant differences in the magnetic ordering of the AF coupled paddle wheels. The lower intensity of the broad, isotropic Lorentzian component indicates improved long-range anti-ferromagnetic ordering. Together with the appearance of a half-field transition (DQ effect) in the powder EPR spectrum a significant, positive influence of the magnetic field on the formation of the EPR silent spin coupled copper dimers is evident. As expected, both phases (MHD and HD only) contain a spectral component due to the presence of mononuclear, extraframework Cu^{+2} compensating the charge of the HPA units enclosed in the pores.[29] The broad, isotropic signal resulting from the inter-dimer interaction between the AF coupled $[Cu\text{-}Cu]^{4+}$ dimers, indicates increased diamagnetism of the phase crystallized in presence of the magnetic field. Because the topology does not change (as confirmed by XRD, Figure S3), enhanced magnetic ordering between the paddle wheels can be concluded. Even without MHD mixing, the interaction between Cu^{2+} and Keggin ion induces dimerization of Cu^{2+} improving the formation of $Cu_3(BTC)_2.3H_2O$, allowing room temperature formation as opposed to the typical hydrothermal synthesis of HKUST-1.[30] This effect is clearly enhanced by the presence of the magnetic field, during the MHD synthesis. The half-field resonance in the EPR spectra of the MHD synthesized sample results from a 'formally' forbidden double quantum coherence in a thermally populated triplet state. The magnetic treatment during self-assembly of the material clearly affects the efficiency of this coherence transfer. A similar half-field transition was observed by Veber et al. studying a temperature induced phase spin transition inducing a diamagnetic dilution of $Cu(hfac)_2LMe$.[31] It should be noted that the 111 planes in the $Cu_3(BTC)_2.3H_2O$ structure resembles a Kagomé lattice with AF coupled Cu^{2+} pairs located on the corners of each triangle (Figure 3, inset right). Since Kagomé lattices count among the geometrically most frustrated magnetic systems,[32] the strong effect of relatively small magnetic fields becomes less surprising.

Magnetic field effects (MFEs) have been reported on chemical reactions with unpaired, spin correlated bi-radicals. MFEs can occur whenever radical pairs structurally or kinetically evolve differently, depending on their spin state (Singlet, $|S_0\rangle$ or Triplet, $|T_0\rangle,|T_{-1}\rangle,|T_{+1}\rangle$) (see Justification SI-1).[33–38] In contrast with the score of studies investigating MFEs in systems with geminal singlet or triplet-born strongly correlated radical pairs,[35,38–41] (e.g. created using laser flash photolysis), almost no research has been performed on MFE's involving initially uncorrelated species, e.g. dissolved paramagnetic metal ions or radicals.[42,43] Because inter system crossing (ISC) is typically much longer lived than diffusional migration of free radicals, such MFEs most often have been observed in micelle systems or systems with increased viscosity where cage reactions increase the lifetime of spin correlated radical pairs.[44,45]

Lifetimes of interacting spin systems are significantly increased when consisting of uni-molecular bi-radicals, micelles or in viscous solvents while spin polarization occurs via fast reactions. The MFEs described in this manuscript all occur in systems with initially uncorrelated paramagnetic ions forming AF coupled spin pairs during synthesis. Consideration of collisional spin pairing statistics readily indicates the importance of S-T ISC during formation of such spin coupled dimers with singlet ground states.[46,47] Since all examples describe solids formed during the MHD treatment, diffusion is expected to be limited, at least on local scale.

The lifetime of spin pairs adsorbed on the surface of the solid phase is probably sufficient to allow ISC, as demonstrated by NMR signal amplification by reversible exchange (NMR-SABRE), where reversible sorption of para-hydrogen in low magnetic field enables the transfer of spin polarization to a substrate which becomes hyperpolarized without chemical modification.[48] Furthermore, a surface can generate local

magnetic field gradients, demonstrated to be beneficial for ISC enhancement.[49–51]

Magnetic Field Effects on Material Formation: The present observations have some similarity with the influence of relatively weak magnetic fields on the ratio between the $CaCO_3$ allotropes calcite and aragonite.[52–55] Weak magnetic fields are also exploited to improve the quality of silicon and germanium single crystals grown by the Czochralski process.[56] Funasako et al. demonstrated how a weak external magnetic field (< 1T), applied during room temperature crystallisation of a paramagnetic ionic liquid induced long range magnetic order in the obtained ferrocenium.[57]

The present observation of MDH assisted self-assembly of VO_x nanoscrolls and MnO_2 nanotubes with topologically periodic spin systems hints at the following underlying mechanism. Precursors with long-lived collective spin states are formed during the MHD treatment, and subsequently assembled during the hydrothermal treatment. The interacting (supra-)molecular precursor species will experience resonance of motion frequencies due to recirculation flow rate and the magnetic field. The resonance envelope is system-dependent as a result of sample specific anisotropic interactions with the MHD constraints. Given that for three different systems a clear MHD effect was observed, the parameter space for obtaining the MHD resonance is quite broad and can most probably be transferred experimentally to many other systems. Reproduction of the reported observations will not depend on limited variation of the magnetic field and hydrodynamic conditions, while fine-tuning of flow and magnetic field of course will have to be performed for each material and experimental setup.

While experimental evidence for impact of magnetic fields on self-assembly under hydrodynamic conditions is accumulating, the theoretical framework remains elusive.[58,59] A priori prediction of the final outcome is currently beyond reach due to the lack of analytical solutions for the mathematical expressions and the much too large computation times for purely numerical approaches describing such resonant systems.

The most comprehensive experimental realisation of long lived hyperpolarized spin states of weak magnetic order can be recognized in the interacting pairs of AF coupled spins in the $[Cu\text{-}Cu]^{4+}$ paddle wheel dimers found in the present MHD synthesized COK-16. It reminds of singlet long lived states of a pair of coupled spins ½ in hyperpolarization approaches to magnetic resonance. Though the long lived singlet states observed and experimentally used in NMR are within reach of theoretical treatment of a pair of spins, for collective spin assemblies theoretical methodologies have not yet been implemented to allow full treatment within current computability limits. A new paradigm for coarser grain computational algorithms must become available before theoretical treatment in large-scale chemical systems could be achieved.

In contrast with the current limitations of theoretical treatment, the role of turbulent flow and magnetic field are confirmed to be related to field orientation, perpendicular to the flow, the flow speed, and the time of exposure to the magnetic field, with an additional internal fluctuation time determined by the weak inter-spin couplings. These four parameters not only control suppression of convection and decreased self-diffusion, resulting in an increase of residence time in collectively migrating density fluctuations, but also determine the timescale and frequency of exposure to the external magnetic field.

The simplicity of the presented experimental MHD device and the resulting control over the critical parameters, flow, magnetic field and total residence time in the magnetic field allows systematic experimental exploration of many systems within rigorously controlled physico-chemical conditions. Extension of the current device with frequency controlled alternating magnetic fields will also enable exploration of weak inter-spin coupling by tuning the devices resonant mode to the fluctuating internal inter-spin fluctuations.

In summary, this report describes how magnetically enhanced hydrodynamic synthesis significantly improves self-assembly and crystallisation of technologically and economically relevant materials containing interacting spin coupled paramagnetic metal ions. Asides increasing efficiency of the synthesis, the magnetic field permanently and drastically improves magnetic order in the material. The simplicity and versatility of the MHD strategy already enables its application for innovation of material synthesis processes and identification of materials potentially hosting long lived polarised spin states.

Similar to simple crystallisation, self-assembly in dynamic systems remains almost terra incognita because of the difficulty to measure and assess proper phenomena governing the transition from density fluctuation to crystallization. The presented magneto hydrodynamic (MHD) strategy enables the development of a new class of devices providing control over parameters that were considered out of reach of manipulation: suppression of self-diffusion, time length of coherent collective behaviour, time window of induction spin order. Nucleation, crystallization and morphological control are therefore accessible with a much broader range of physico-chemical controls for elucidating complex many-body spin systems that resisted advanced investigation up to now.

Although a general framework explaining the generation of long lived spin states and their impact during magnetically enhanced material synthesis is developing very fast, further improvements will be dependent upon experimental categorization of the score of physicochemical parameters potentially affecting this process needs to be simplified by experimental categorization derived from by systematic observations for different chemical systems. The development of inter-spin coupling of pairs in the different schemes of hyperpolarization in NMR can impact deeply the description of these long lived magnetic, albeit at a cost of developing a new generation of theoretical models for description of multi-spin magnetic interactions. As a result the presented results can be expected to stimulate the exploitation of the magnetic field effects on material synthesis, and also to induce further developments in spectroscopies exploiting spin polarization.

Experimental Section

Manganese oxide nanotubes were prepared in the MHD system describe above, using a synthesis recipe described in literature.[21] Potassium permanganate (0.39 g, $KMnO_4$) was mixed with hydrochloric acid (0.82 mL, 37 %) in distilled water (45 mL). The resulting mixture was aged for 10 minutes in the MHD system at a flow rate of 4 L/min, respectively in absence and presence of the external magnetic field. The

final products were obtained after hydrothermal treatment at 140 °C for 12 h, dried in a vacuum oven overnight (40 °C).

Vanadium oxide nanoscroll synthesis was done by mixing solvent (42 mL, EtOH/H_2O = ½ vol/vol), V_2O_5 (6.68 g, 36.73 mmol) and dodecylamine (4.92 g, 26.54 mmol), corresponding to a surfactant-to-vanadium ratio of 0.36. The mixture (total volume: 50 mL) was filled in the tubing of the MHD system and aged at room temperature for 6 h at 4 L/min respectively in absence and presence of the external magnetic field oriented orthogonally to the flow direction. The resulting gel was transferred into a Teflon-lined autoclave (23 mL volume) and hydrothermally treated for 3 days at 180°C. The as-synthesized nanotubes were filtered, washed with EtOH and hexane and also dried under vacuum.

HKUST-1 type MOF COK-16 was prepared by dissolution of $Cu(NO_3)_2.3H_2O$ (Fluka) in a $H_3PW_{12}O_{40}$ (Fluka) solution (10^{-3} M) prepared using a 50% vol. ethanol (VWR)-water solution containing $NaNO_3$ (0.1 M). Upon complete dissolution, a 1,3,5-H_3BTC (Acros organics) solution (1.259×10^{-2} M) prepared from 50% vol. ethanol-water containing $NaNO_3$ (0.1 M) was added. After mixing the pH of all synthesis solutions was 3±0.1. 50 ml of this synthesis mixture was transferred to a transparent tube (Masterflex High Perfomance Tygon 70 Lab tubing R-3603, with 8 mm inner diameter and total volume of 50 ml) equipped with a magneto hydrodynamic device and pumped at RT in a peristaltic pump (Cole Parmer High Performance Pump – Model I/P 77600-62) applying a flow rate of 4 L/min respectively in absence and presence of an external magnetic field (NdFeB block magnets, B = 0.3 T) oriented orthogonally to the flow direction.

A detailed experimental description of the material characterisation is given in the Supporting Information.

Supporting Information

Supporting Information is available from the Wiley Online Library or from the author.

Acknowledgements

J. Maes, S. Usé and W. Wouters are gratefully acknowledged for their continuous technical assistance. J.E and E.B. wish to acknowledge fruitful discussions with J. Vanacken. S.R.B thanks Dr. Arunakumar for initial discussions. We are grateful to Amudhakumari for constant help with literature. M. Seo and N. de Greef are kindly acknowledged for their assistance with initial TEM measurements on the manganese and vanadium oxide nanotubes, E. Gobechiya for assistance with PXRD measurements.

Author Contributions – E.B. designed the research plan, performed EPR characterisation and prepared the manuscript. J.E. contributed to the experimental design, synthesis and characterization of V/Mn nanotubes. D.M. and S.R.B worked on COK-16 synthesis. T.A and K.V.H. performed the TEM/tomography activities coordinated by S.B. and G.V.T. F.T and C.E.A.K contributed to the structural characterisation and to the interpretation of the results. J.A.M initiated and supported weak magnetic field assisted synthesis research. All authors assisted in the writing of the publication and have given approval to the final version of the manuscript.

Funding Sources – We thank the Flemish Government for long-term structural funding (Methusalem). E.B. acknowledges the Flemish FWO for a postdoctoral fellowship. J.E. acknowledges financial support by the "Institute for the Promotion of Innovation through Science and Technology in Flanders (IWT-Vlaanderen)". G.V.T. and S.B. acknowledge financial support from the European Research Council (ERC Advanced Grant # 24691-COUNTATOMS, ERC Starting Grant #335078-COLOURATOMS) and the Integrated Infrastructure Initiative N. 262348 European Soft Matter Infrastructure, ESMI. S.R.B acknowledges financial support from the European Commission via an FP7 Marie Curie (IEF) fellowship. The Flemish government is acknowledged for long-term structural funding (Methusalem) and the Belgian government for financing interuniversity poles of attraction (IAP-PAI). F.T. thanks KULeuven BOF for a SF fellowship.

Received: February 21, 2014
Revised: April 23, 2014
Published online: June 2, 2014

[1] A. F. Demirörs, P. P. Pillai, B. Kowalczyk, B. Grzybowski, *Nature* **2013**, *503*, 99.
[2] S. Tantrawong, C. Engkagul, *Thammasat Int. J. Sci. Tech.* **1998**, *3*, 1.
[3] M.-R. Gao, S.-R. Zhang, Y.-F. Xu, Y.-R. Zheng, J. Jiang, S.-H. Yu, *Adv. Funct. Mater.* **2014**, *24*, 916.
[4] A. Bricard, J.-B. Caussin, N. Desreumaux, O. Dauchot, D. Bartolo, *Nature* **2013**, *503*, 95.
[5] G. M. Whitesides, B. Grzybowski, *Science* **2002**, *295*, 2418.
[6] M.-J. Hu, Y. Lu, S. Zhang, S.-R. Guo, B. Lin, M. Zhang, S.-H. Yu, *J. Am. Chem. Soc.* **2008**, *130*, 11606.
[7] Y. Lu, Y. Zhao, L. Yu, L. Dong, C. Shi, M.-J. Hu, Y.-J. Xu, L.-P. Wen, S.-H. Yu, *Adv. Mater.* **2010**, *22*, 1407.
[8] B. Grzybowski, H. Stone, G. Whitesides, *Nature* **2000**, *405*, 1033.
[9] J. M. D. Coey, R. Aogaki, F. Byrne, P. Stamenov, *Proc. Natl. Acad. Sci. USA* **2009**, *106*, 8811.
[10] M. S. Tillack, N. B. Morley, in *Standard Handbook for Electrical Engineers* (Eds.: D. G. Fink, H. W. Beaty), McGraw-Hill, New York, **1998**, p. 88.
[11] S. Kerkhofs, H. Lipkens, F. Velghe, P. Verlooy, J. A. Martens, *J. Food Eng.* **2011**, *106*, 35.
[12] B. Stuyven, G. Vanbutsele, J. Nuyens, J. Vermant, J. A. Martens, *Chem. Eng. Sci.* **2009**, *64*, 1904.
[13] B. Stuyven, Q. Chen, W. Van De Moortel, H. Lipkens, B. Caerts, A. Aerts, L. Giebeler, B. Van Eerdenbrugh, P. Augustijns, G. Van Den Mooter, J. Van Humbeeck, J. Vanacken, V. V Moshchalkov, J. Vermant, J. A. Martens, *Chem. Commun.* **2009**, *0*, 47.
[14] B. Stuyven, J. Emmerich, P. Eloy, J. Van Humbeeck, C. E. A. Kirschhock, P. A. Jacobs, J. A. Martens, E. Breynaert, *Appl. Catal. A Gen.* **2014**, *474*, 18.
[15] J. C. Richard, *J. Comput. Nonlinear Dyn.* **2013**, *8*, 031010.
[16] G. Ertl, *Science* **1991**, *254*, 1750.
[17] G. Ertl, *Angew. Chem. Int. Ed. Engl.* **2008**, *47*, 3524.
[18] Y. Muraoka, H. Chiba, T. Atou, M. Kikuchi, K. Hiraga, Y. Syono, S. Sugiyama, S. Yamamoto, J.-C. Grenier, *J. Solid State Chem.* **1999**, *144*, 136.
[19] J. Luo, H. T. Zhu, H. M. Fan, J. K. Liang, H. L. Shi, G. H. Rao, J. B. Li, Z. M. Du, Z. X. Shen, *J. Phys. Chem. C* **2008**, *112*, 12594.
[20] J. Luo, H. T. Zhu, J. K. Liang, G. H. Rao, J. B. Li, Z. M. Du, *J. Phys. Chem. C* **2010**, *114*, 8782.
[21] W. Xiao, H. Xia, J. Y. H. Fuh, L. Lu, *J. Power Sources* **2009**, *193*, 935.
[22] R. Zeng, J. Q. Wang, W. X. Li, G. D. Du, Z. X. Chen, S. Li, S. X. Dou, **2012**.
[23] J. Emmerich, E. Breynaert, C. E. A. Kirschhock, J. A. Martens, *Catal. Today* **2012**, *192*, 63.
[24] H. Kweon, K. W. Lee, C. E. Lee, *J. Appl. Phys.* **2010**, *108*, 023905.
[25] J. Livage, *Materials (Basel)*. **2010**, *3*, 4175.
[26] X. Commeinhes, P. Davidson, C. Bourgaux, J. Livage, *Adv. Mater.* **1997**, *9*, 900.
[27] A. van der Est, M. Asano-Someda, P. Ragogna, Y. Kaizu, *J. Phys. Chem. A* **2002**, *106*, 8531.
[28] P. Y. Zavalij, M. S. Whittingham, *Acta Crystallogr. Sect. B Struct. Sci.* **1999**, *55*, 627.
[29] S. R. Bajpe, E. Breynaert, A. Martin-Calvo, D. Mustafa, S. Calero, C. E. A. Kirschhock, J. A. Martens, *ChemPlusChem* **2013**, *78*, 402.

[30] S. R. Bajpe, E. Breynaert, D. Mustafa, M. Jobbágy, A. Maes, J. A. Martens, C. E. A. Kirschhock, *J. Mater. Chem.* **2011**, *21*, 9768.
[31] S. L. Veber, M. V Fedin, K. Y. Maryunina, G. V Romanenko, R. Z. Sagdeev, E. G. Bagryanskaya, V. I. Ovcharenko, *Inorganica Chim. Acta* **2008**, *361*, 4148.
[32] J. L. Atwood, *Nat. Mater.* **2002**, *1*, 91.
[33] K. M. Salikhov, Y. N. Molin, R. A. Sagdeev, A. L. Buchachenko, *Spin Polarization and Magnetic Field Effects in Radical Reaction*, Elsevier, **1984**.
[34] $|S_0\rangle = 1/\sqrt{2}(|\alpha\beta\rangle - |\beta\alpha\rangle)$; $|T_{+1}\rangle = |\alpha\alpha\rangle$; $|T_0\rangle = 1/\sqrt{2}(|\alpha\beta\rangle + |\beta\alpha\rangle)$; $|T_{-1}\rangle = |\beta\beta\rangle$
[35] C. T. Rodgers, *Pure Appl. Chem.* **2009**, *81*, 19.
[36] K.-N. Hu, H. Yu, T. M. Swager, R. G. Griffin, *J. Am. Chem. Soc.* **2004**, *126*, 10844.
[37] A. Abragam, M. Goldman, *Reports Prog. Phys.* **1978**, *41*, 395.
[38] C. R. Timmel, K. B. Henbest, *Philos. Trans. R. Soc. London, Ser. A Math. Phys. Eng. Sci.* **2004**, *362*, 2573.
[39] K. Schulten, A. Weller, *Biophys. J.* **1978**, *24*, 295.
[40] Y. Sakaguchi, *Mol. Photochem.* **2002**, *46*, 18.
[41] U. Werner, Y. Sakaguchi, H. Hayashi, G. Nohya, R. Yoneshima, S. Nakajima, A. Osuka, *J. Phys. Chem.* **1995**, *99*, 13930.
[42] G. Ferraudi, *J. Phys. Chem.* **1993**, *97*, 11929–11936.
[43] W. Schlenker, T. Ulrich, U. E. Steiner, *Chem. Phys. Lett.* **1983**, *103*, 118.
[44] K. Lüders, K. M. Salikhov, *Chem. Phys.* **1987**, *117*, 113.
[45] A. R. O'Dea, A. F. Curtis, N. J. B. Green, C. R. Timmel, P. J. Hore, *J. Phys. Chem. A* **2005**, *109*, 869.
[46] Z. Schulten, K. Schulten, *J. Chem. Phys.* **1977**, *66*, 4616.
[47] D. Canet, C. Aroulanda, P. Mutzenhardt, S. Aime, R. Gobetto, F. Reineri, *Concepts Magn. Reson. Part A* **2006**, *28A*, 321.
[48] R. W. Adams, J. A. Aguilar, K. D. Atkinson, M. J. Cowley, P. I. P. Elliott, S. B. Duckett, G. G. R. Green, I. G. Khazal, J. López-Serrano, D. C. Williamson, *Science* **2009**, *323*, 1708.
[49] M. C. D. Tayler, M. H. Levitt, *Phys. Chem. Chem. Phys.* **2011**, *13*, 9128.
[50] M. Carravetta, M. H. Levitt, *J. Chem. Phys.* **2005**, *122*, 214505.
[51] H. Lee, N. Yang, A. E. Cohen, *Nano Lett.* **2011**, *11*, 5367.
[52] Z. Zhang, Y. Xie, X. Xu, H. Pan, R. Tang, *J. Cryst. Growth* **2012**, *343*, 62.
[53] S. Knez, C. Pohar, *J. Colloid Interface Sci.* **2005**, *281*, 377.
[54] F. Alimi, M. Tlili, M. Ben Amor, C. Gabrielli, G. Maurin, *Desalination* **2007**, *206*, 163.
[55] J. S. Baker, S. J. Judd, *Water Res.* **1996**, *30*, 247.
[56] K. Kakimoto, M. Eguchi, H. Ozoe, *J. Cryst. Growth* **1997**, *180*, 442.
[57] Y. Funasako, T. Mochida, T. Inagaki, T. Sakurai, H. Ohta, K. Furukawa, T. Nakamura, *Chem. Commun.* **2011**, *47*, 4475.
[58] M. Mastrangeli, S. Abbasi, C. Varel, C. Van Hoof, J.-P. Celis, K. F. Böhringer, *J. Micromech. Microeng.* **2009**, *19*, 83001.
[59] N. B. Crane, O. Onen, J. Carballo, Q. Ni, R. Guldiken, *Microfluid. Nanofluidics* **2012**, *14*, 383.